Dynamic Model Analysis of a Pneumatically Operated Flexible Arm

FERNANDO F. KIYAMA
Depto. de Diseño y Desarrollo de Equipo
CRODE-Chihuahua
Homero 350 Chihuahua, Chih. 31109
MÉXICO
fkiyamam@yahoo.com.mx

EMILIO VARGAS
Laboratorio de Mecatrónica
CIDESI-Querétaro
Playa Pie de la Cuesta 702 Querétaro, Qro. 76130
MÉXICO
emilio@mecatronica.net

Abstract: - This paper is about the model analysis of one of the degrees of freedom of an industrial flexible manipulator, pneumatically operated by means of a cushion type air cylinder. Pneumatic modelling is made upon the thermodynamic principles of mass and energy conservation, and the actuator hybrid state nature analyzed. The flexible arm model is made using constrained generalized coordinates, and the assumed modes method. Vibration modes contribution to the response is compared with experimental data. The manipulator structural controllability and observability are considered by means of its structure graph.

Key-Words: - Flexible manipulator, pneumatic cylinder, actuator, modelling, state transitions, controllability, observability, graph.

1 Introduction

Some particular systems, such as light industrial manipulators and the large space structures require lightweight elements. Weight reduction however, results in lack of sensing, vibration, and incapability of precise positioning because of the flexibility of the system, and difficulty to obtain accurate model.

Additionally pneumatic actuators have advantages such as low cost, clean operation and high power to weight ratio that favor their potential use in robotic systems to achieve slender, light, simple and economic manipulators. In the other hand pneumatic actuators control is problematic because of their highly nonlinear characteristics.

Flexible manipulator modelling, has been done for many years to describe its dynamic behavior and improving it. Several methods have been proposed to consider the effect of elasticity. One is the assumed modes method [1], [2], [3]. Another is the finite element method [4], [5]. A third method commonly adopted by many researchers, is the lumped parameter method [6], [7].

The development of digital control has promoted the research of pneumatic servo systems [8] and as an alternative the pulse-width modulated control (PWM) [9]

Since modelling of flexible manipulators is very complex, many researches consider as a first step only one link as flexible [7], [5]. Nevertheless powerful computers have enabled to consider several links to be flexible [1], [2], [3], [4], [6].

Pneumatic servo systems development require the modelling and simulation tools for their design and for the components evaluation and selection [10]. Anglani et al [11] have developed the simulation enviroment for actuators under the PWM scheme.

This work is about the model analysis of one of the degrees of freedom, for an industrial type flexible manipulator, operated by a pneumatic cylinder equipped with break cushions. The elasticity of the arm is modelled using constrained generalized coordinates and the assumed modes method. The description of the dynamics of the control valve and the linear actuator is presented, and its hybrid state nature analyzed by means of state transition graphs. Vibration modes contribution to the response is considered and compared with experimental data. Controllability and observability are considered from structural notions [13] and for this purpose the manipulator structure graph is presented.

This work is part of the development on an industrial dielectric manipulator, designed for the cleaning maintenance of insulators in electric power lines, [12].

2 System Description

The system is actuated by a single-rod double action pneumatic cylinder $64\,mm$ in diameter and $102\,mm$ stroke, equipped with brake cushions to

limit the speed of the piston, that could damage itself when it bumps the cylinder extremities.

Details of the manipulator arm construction are shown in figure 1. It is driven, by means of a kinematic chain formed by the pneumatic cylinder, as a slider-crank mechanism pinned to a rigid four bar mechanism. The arm structure consists of a rigid base and a 27 mm PVC pipe, 1.5 m long, which actually is a two link chain operating in the vertical plane.

The air flow is regulated by two free return needle valves and the air direction is controlled with a three position, closed center directional valve, the timed opening and closing sequence of this valve is preprogrammed in LabVIEW, where several key variables are also recorded.

The instrumentation considered to measure the prototype response is as follows: pressure sensors for each of the two cylinder ports, a load cell attached to the piston rod, and a potentiometer to record the flexible arm base position. The arm vibration is measured with eight strain gage half bridges glued along the arm.

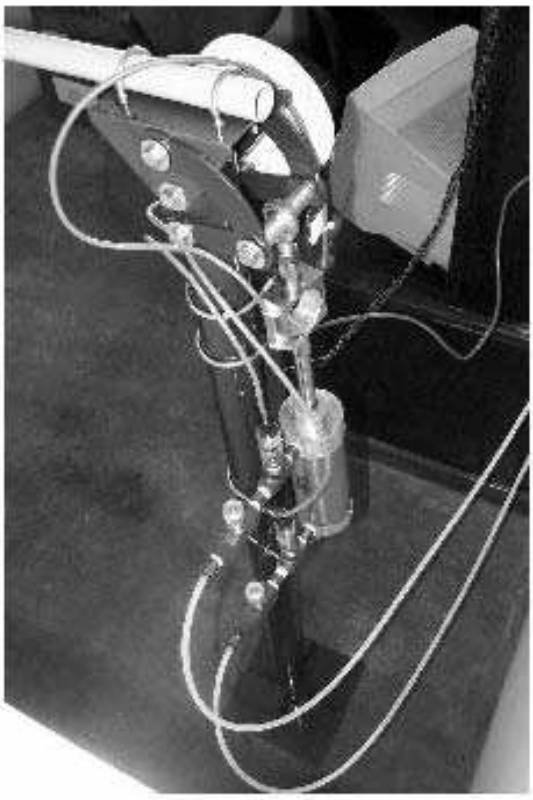

Fig. 1 Experimental arrangement of the flexible manipulator.

3 System Variables

The vector variables considered in the system model are as follows:

3.1 State Vector

The state vector includes the pressure chambers as described in figure 2, the position θ_6 and velocity $\dot{\theta}_6$ of the arm base and the coordinates associated with the arm vibration as described in figure 3:

$$p = [p_{a1}\, p_1\, p_2\, p_{a2}\, \theta_6\, \dot{\theta}\, q_1\, q_2\, \dot{\theta}_6\, \dot{\theta}\, \dot{q}_1\, \dot{q}_2]^T \qquad (1)$$

3.2 Input Vector

The input is comprised by the inlet and outlet valve area openings:

$$u = [a_1\, a_2\, a_o]^T \qquad (2)$$

where a_1 and a_2 are the valve inlets for the piston and rod sides of the cylinder respectively and a_o is the valve outlet.

3.3 Measured Output

The variables considered for the measured output vector are those that were instrumented to be sensed on the test prototype:

$$y = [p_{a1}\, p_{a2}\, F_v\, \theta_6\, v]^T \qquad (3)$$

where p_{a1} and p_{a2} are the pressures as measured at the cylinder ports, F_v is the piston force, θ_6 is the arm base position and v is flexible arm tip vibration.

4 Model Equations

The manipulator model is comprised by the actuator and the elastodynamic models of the flexible arm.

4.1 Hybrid Approach

The pneumatic parts of the system exhibit discrete behavior. Their dynamics are described by equations that behave as discussed below. This equations refer to a dedicated hybrid state only, so they may change in different domains of the state space.

4.1.1 Flow pattern through the control valve

The valve modelling details can be found in [14]. The mass flow rate depends on the values of the inlet valve pressure p_0, and outlet valve pressure p_1:

$$\dot{m} = C_d\, \gamma \sqrt{\frac{k}{RT_0}}\, p_0\, A_t \qquad (4)$$

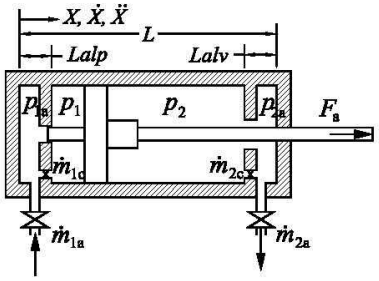

Fig. 2 Pneumatic actuator with cushion chambers.

$$\gamma = \sqrt{\frac{2}{k-1}} \left(\frac{p_t}{p_0}\right)^{\frac{1+k}{2k}} \left[\left(\frac{p_t}{p_0}\right)^{\frac{1-k}{k}} - 1\right]^{\frac{1}{2}} \quad (5)$$

where k and R are the ratio of specific heats c_p/c_v, and the gas constant respectively, T_0 is the inlet temperature, p_t is the valve throat pressure, and C_d is the discharge coefficient.
Depending on the pressure ratio, the flow regime for air can be:

Subcritical Flow $(0,528 < \frac{p_1}{p_0} \leq 1)$ The flow is described by equations 4 and 5.

Critical and Supercritical Flow $(\frac{p_1}{p_0} \leq 0,528)$ When the flow reaches its critical regime, the coefficient γ gets a steady value of 0.5787 that will not change with further decrease of the outlet pressure p_1, therefore the flow state remains constant.

4.1.2 Dynamic relationship within the actuator chambers

The pneumatic actuator is a double-acting linear air cylinder as shown in figure 2.

Depending on the piston position, the rate of change of pressure inside the cylinder chambers, including the cushions as shown in figure 2, can be calculated from the following equations:

If $0 \leq X \leq Lalp$ then

$$\dot{p}_{a1} = \frac{k\,R\,T_0}{A_{ap}\left(X + \frac{\Delta A_p}{A_{ap}}\right)} \left[\dot{m}_{1a} - \dot{m}_{1c} - \frac{A_{ap}}{R\,T_0} p_{a1}\dot{X}\right] \quad (6)$$

$$\dot{p}_1 = \frac{k\,R\,T_0}{(A_p - A_{ap})X} \left[\dot{m}_{1c} - \frac{A_p - A_{ap}}{R\,T_0} p_1\dot{X}\right] \quad (7)$$

If $Lalp < X \leq L$ then

$$\dot{p}_{a1} = \frac{k\,R\,T_0}{A_p(X+\Delta)} \left[\dot{m}_{1a} - \frac{A_p}{R\,T_0} p_{a1}\dot{X}\right] \quad (8)$$

$$\dot{p}_1 = \frac{k\,R\,T_0}{A_p(X+\Delta)} \left[\dot{m}_{1c} - \frac{A_p}{R\,T_0} p_1\dot{X}\right] \quad (9)$$

If $0 \leq X < (L - Lalv)$ then

$$\dot{p}_2 = \frac{k\,R\,T_0}{(A_p - A_r)(L - X + \Delta)} \left[\dot{m}_{2c} + \frac{A_p - A_r}{R\,T_0} p_2\dot{X}\right] \quad (10)$$

$$\dot{p}_{a2} = \frac{k\,R\,T_0}{(A_p - A_r)(L - X + \Delta)} \left[\dot{m}_{2a} + \frac{A_p - A_r}{R\,T_0} p_{a2}\dot{X}\right] \quad (11)$$

If $(L - Lalv) \leq X \leq L$ then

$$\dot{p}_2 = \frac{k\,R\,T_0}{(A_p - A_r)(L - X)} \left[\dot{m}_{2c} + \frac{A_p - A_r}{R\,T_0} p_2\dot{X}\right] \quad (12)$$

$$\dot{p}_{a2} = \frac{k\,R\,T_0}{L - X + \frac{\Delta A_p}{A_{av} - A_v}} \left[\frac{\dot{m}_{2a} - \dot{m}_{2c}}{A_{av} - A_r} + \frac{p_{a2}\dot{X}}{R\,T_0}\right] \quad (13)$$

the development of this set of equations is given in [14].

4.2 Flexible Arm Dynamics

The arm rigid base is pivoted in the origin of the inertial frame XY as shown in Figure 3, the flexible bar is fixed to the rigid base, and attached to a moving reference frame xy.

The Lagrange approach is used to derive the equations of motion for the arm dynamics and the assumed modes method to obtain the discretized form for the elastic displacement, their form can be seen in [15].

4.2.1 The assumed modes

The use of a moving frame to describe the primary motion of the manipulator, introduces the additional variable θ (see Figure 3), which requires an

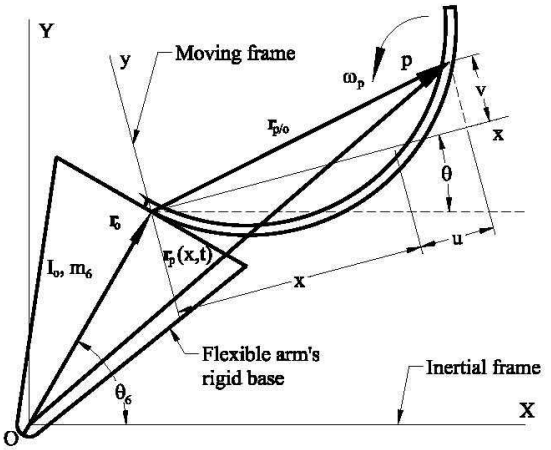

Fig. 3 Arm deformation about inertial coordinates.

additional constraint equation to deal with. The constraint determines the boundary conditions associated with the elastic movement. The adequate selection of assumed modes guarantees the constraint to be satisfied, being equal to choose a set of independent generalized coordinates.

Considering that the rigid base and the flexible arm form an unarticulated unit, it would be natural to consider the zero slope constraint, therefore selecting assumed modes such that the elastic movement has zero slope in the arm's attachment to the base, this allows to express the angular position θ of the moving frame in terms of the angular position θ_6 of the rigid base, rendering simpler equations of motion, unfortunately in this work it was found in practice as [16] indicates, that this constraint leads to an inaccurate model when either one or both of $\dot{\theta}$ and the secondary motion amplitudes $q_1, \ldots, q_n$ increase.

In the model proposed in [15] the rigid body constraint is used, which forces the secondary motion to have no rigid body components. The constraint has the form:

$$\frac{1}{\sqrt{I_0}} \int_0^L \mu \, x \, v(x,t) \, \mathrm{d}x = 0 \tag{14}$$

4.2.2 Differential-algebraic formulation

The model of the flexible manipulator as considered in the previous section represents a two link pined chain, so we introduce a constraint equation to express the perpendicularity between the rigid base position, and the slope of the flexible arm's attachment:

$$\boldsymbol{f}(\boldsymbol{q}) = \left[\frac{\partial \boldsymbol{r}_p}{\partial x}\right]_{x=0} + \frac{1}{\|\boldsymbol{r_0}\|}\frac{\partial \boldsymbol{r_0}}{\partial \theta_6} = 0 \tag{15}$$

Gathering equations of motion together with the constraint 15 becomes the differential-algebraic system shown below:

$$\dot{\boldsymbol{q}} = \boldsymbol{z} \tag{16}$$

$$\boldsymbol{M}(\boldsymbol{q})\dot{\boldsymbol{z}} = \boldsymbol{h}(\boldsymbol{q}, \boldsymbol{z}) - \boldsymbol{F}^T(\boldsymbol{q})\lambda_1 \tag{17}$$

$$0 = \boldsymbol{f}(\boldsymbol{q}) \tag{18}$$

where $\boldsymbol{M}(\boldsymbol{q})$ is the mass matrix, $\boldsymbol{F}(\boldsymbol{q}) = \partial \boldsymbol{f}/\partial \boldsymbol{q}$, $\boldsymbol{q} = \{\theta_6, \theta, q_1, \ldots, q_n\}^T$, $\boldsymbol{z} = \{\dot{\theta}_6, \dot{\theta}, \dot{q}_1, \ldots, \dot{q}_n\}^T$ and λ_1 is the Lagrange multiplier.

5 Dynamic Model Analysis

The discrete behavior of the pneumatic components described in equations 4 through 13 can be adequately analyzed by means of a state transition graph.

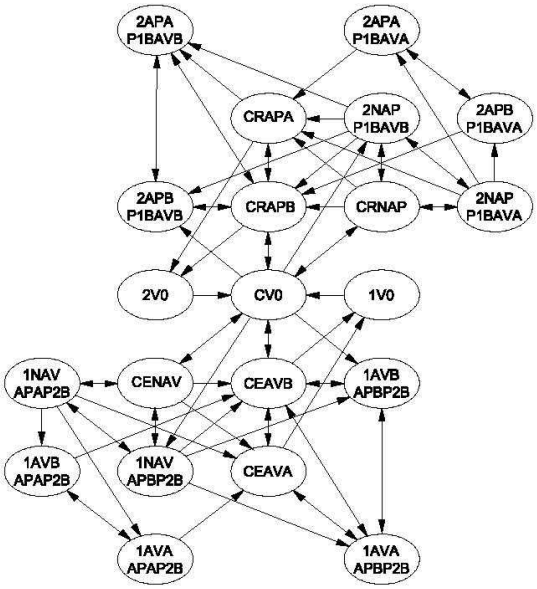

Fig. 4 State transitions diagram for the pneumatic actuator.

5.1 Hybrid State Transitions

The pneumatic actuator model includes the property that state functions are picewise defined depending on pressure values and the relative position between the actuator cylinder and piston. These hybrid states define smooth state functions on the boundary of the corresponding hybrid domain in at least first order.

The pneumatic actuator state transitions are shown in Figure 4. The properties of these hybrid states can be summarized as follows:

- The initial CR labelled states refer to closed control valve, return movement conditions.
- The initial CE labelled states refer to closed control valve, extending movement conditions.
- The initial 1 labelled states refer to pressure P1 on the piston side actuator port.
- The initial 2 labelled states refer to pressure P2 on the rod side actuator port.
- The AP refers to the piston cushion and NAP to the rest of the stroke.
- The AV refers to the rod cushion and NAV to the rest of the stroke.
- The V0 refers to the states where the piston is in still position.
- The B refers to subsonic streaming property in the related chamber.

Table 1: Errors for the first four modes

Parameter	$\phi_1 q_1$	$\sum_{i=1}^{2} \phi_i q_i$	$\sum_{i=1}^{3} \phi_i q_i$	$\sum_{i=1}^{4} \phi_i q_i$
$\mathcal{E}_{p_{a1}}$	0.0316	0.0218	0.0182	0.0162
$\mathcal{E}_{p_{a2}}$	0.0299	0.0232	0.0212	0.0205
$\mathcal{E}_{F_r}$	1.0875	0.5681	0.5043	0.4924
$\mathcal{E}_{\theta_6}$	8.1354	8.1337	8.1334	8.1323
$\mathcal{E}_v$	2.0990	2.0658	2.0604	2.1222
$\mathcal{E}_{tot}$	8.4720	8.4112	8.4055	8.4191

- The A refers to sonic streaming property in the related chamber.

The state transition graph shows that the states form a strongly connected components in themselves, therefore the system is reachable without deadlocks, cyclic behavior or conflict situations.

5.2 Modes Contribution

For beams, the modes contribution to the response is known to fall faster than for elements vibrating in tension or torsion [17]. To investigate the modes contribution, simulation results obtained with different number of modes is compared with the experimental data, using the following metrics:

$$\mathcal{E} = \sqrt{\frac{\sum_{i=1}^{n}[(d_s - d_e)/\bar{d}]^2}{N}} \tag{19}$$

where d_s and d_e are simulation and experimental results respectively, $\bar{d}$ is the mean of d_e and N is the amount of data. Results for the first four modes are shown in table 1. The global error $\mathcal{E}_{tot}$ is calculated from gathering the errors obtained for each of the measured output variables:

$$\mathcal{E}_{tot} = \sqrt{\mathcal{E}_{p_{a1}}^2 + \mathcal{E}_{p_{a2}}^2 + \mathcal{E}_{F_r}^2 + \mathcal{E}_{\theta_6}^2 + \mathcal{E}_v^2} \tag{20}$$

Table 1 shows a continuous diminishing of errors with the increasing number of modes employed, for all parameters but $\mathcal{E}_v$ and consequently $\mathcal{E}_{tot}$ that jump for the four modes model.This is due to the fact that for each of the first three models there is a slight vibration frequency difference between simulation and experiment that makes both responses match for some periods diminishing the error, but for the four modes model there is a steady phase difference, resulting in a bigger error.

The results suggest that the most significant error diminishment is accomplished considering a two modes model.

5.3 Structural Controllability and Observability

The nonlinear local controllability in the neighborhood of an operation point $\boldsymbol{p}_0$ is verified by means of the controllability distribution of the system [18]. Considering the complexity of the state matrix and its hybrid characteristics, controllability is considered here by structural properties.

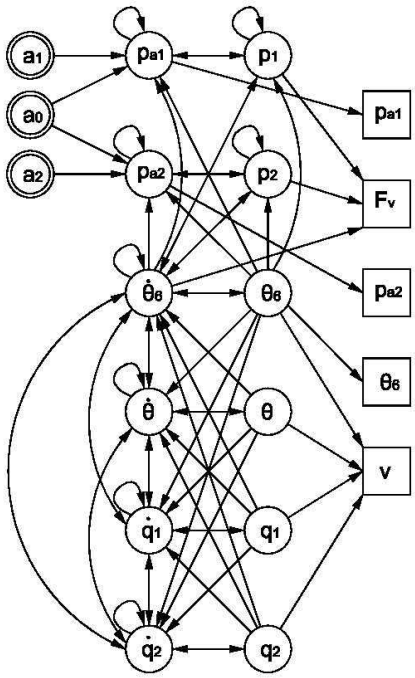

Fig. 5 Flexible manipulator structure graph.

According with equations 1, 2 and 3, the structure indices of the system variables are:

$$\boldsymbol{p} \in \Re^{12},\ \boldsymbol{y} \in \Re^{5},\ \boldsymbol{u} \in \Re^{3} \tag{21}$$

therefore the dimension of structure matrices, for the model linearization as defined by the above structure indices are:

$$[\boldsymbol{A}] \in \Re^{13\times 12},\ [\boldsymbol{C}] \in \Re^{5\times 12},\ [\boldsymbol{B}] \in \Re^{13\times 3} \tag{22}$$

where 13 rows are considered for matrixes $[\boldsymbol{A}]$ and $[\boldsymbol{B}]$ because of the addition of the restriction equation. The structure graph of the flexible manipulator is constructed from the structure indices and structure matrices and shown in figure 5.

If only the structure of the system is given, then the notion of structural controllability or observability is used, according with the following [13]:

Theorem 1 *A linear system with structure matrices ($[\boldsymbol{A}]$,$[\boldsymbol{B}]$,$[\boldsymbol{C}]$)is structurally controllable or observable if*

1. *the matrix $[\boldsymbol{A}]$ is of full structural rank, and*
2. *the system structure graph S is input connectable or output connectable.*

The system structure graph describes the complete interaction between the entries of the system variables, therefore besides the full structural rank property of the structure matrix $[\boldsymbol{A}]$, it is checked in figure 5 for controllability, the existence of at least one directed path from any of the input variables to each of the state variables, and for observability the existence of at least one directed path form each of the state variables to one of the output variables.

6 Conclusion

The hybrid nature of the pneumatic actuator, represented by its state transitions was studied founding that the system is reachable without deadlocks, cyclic behavior or conflict situations.

Comparison of simulation results and experimental data shows that significant error diminishing in the response occurs for the first two modes for this particular model and operating range.

From model linearization, the system controllability and observability are considered on behalf of the full structural rank of the state matrix and the existence in the structure graph, of direct paths from the input variables to the state variables for controllability and from the state variables to the output variables for observability.

References:

[1] W. J. Book, *Recursive Lagrangian Dynamics of Flexible Manipulator Arms*, International Journal of Robotics Research, Vol. 3, No 3, 1984, pp 87-101.

[2] H. Baruh and S. S. K. Tadikonda, *Issues in the Dynamics and Control of Flexible Robot Manipulators*, Journal of Guidence, Control, and Dynamics 12, No 5, 1989, pp 659-671.

[3] W. J. Book and K. Obergfell *Practical Models for Practical Flexible Arms*, Proceeding of the 2000 IEEE International Conference on Robotics & Automatition, 2000.

[4] P. B. Usoro, R. Nadira and S. S. Mahil, *A Finite Element/Lagrange Approach to Modeling Lightweight Flexible Manipulators*, Journal of Dynamic Systems, Measurement and Control, Vol. 108, Sept. 1986, pp. 198-205.

[5] M. O. Tokhi, Z. Mohamed, S. H. M. Amin and R. Mamat, *DYNAMIC CHARACTERISATION OF A FLEXIBLE MANIPULATOR SYSTEM: THEORY AND EXPERIMENTS*, TENCON 2000. Proceedings, Volume: 3, Sept. 2000, pp. 167-172.

[6] T. Yoshikawa and K. Hosoda, *Modeling of flexible Manipulators Using Virtual Rigid Links and Passive Joints*, IEEE/RSJ International Workshop on Intelligent Robots and Systems, Nov. 1991, pp. 967-972.

[7] J. J. Feliu, V. Feliu and K. C. Cerrada, *Load Adaptative Control of Single-Link Flexible Arms Based on a New Modeling Technique*, IEEE Transactions on Robotics and Automation, Vol. 15, No 5,Oct. 1999, pp. 793-804.

[8] S. Ning, and G. M. Bone, *High Steady-State Accurate Pneumatic Servo Positioning Systems with PVA/PV Control and Friction Compensation*, Proceedings of the 2002 IEEE International Conference on Robotics and Automation. Washington, DC. May 2002.

[9] E. J. Barth, J. Zhang and M. Goldfarb, *Sliding Mode Approach to PWM-Controlled Pneumatic Systems*, Proceedings of the American Control Conference. Anchorage, AK. May 2002.

[10] P. Moore and J. Sheng, *Pneumatic servo actuator technology*, IEE Colloquium: Actuator Technology: Current practice and new developments, London. May 1996.

[11] A. Anglani, D. Gnoni A. Grieco and M. Pacella. *A cad enviroment for numerical simulation of servo pneumatic actuator systems*, AMC 2002, Maribor, Slovenia. 2002, pp 593-598.

[12] E. Vargas, G. Reynoso, L. Villareal and R. Mier, *Diseño de un robot industrial para aplicaciones de limpieza en subestaciones eléctricas*, 3er Congreso Mexicano de Robótica, Querétaro. Asociación Mexicana de Robótica,Sept. 2001.

[13] K. M. Hangos, and I. Cameron *Process Modelling and Model Analysis*, Process systems engineering Volume 4, Academic Press, London. 2001

[14] F. F. Kiyama y E. Vargas *Modelo Termo-Mecánico para un Manipulador Tipo Dieléctrico*, INFORMACIÓN TECNOLÓGICA. Vol 15, No 5, 2004, pp 23-31

[15] F. F. Kiyama y E. Vargas *Modelling of a Single Degree of Freedom Flexible Arm Pneumatically Operated*, International Symposium on Robotics and Automation ISRA 2004-09-23 Querétaro, Qro.Aug. 2004, pp. 218-225.

[16] H. Baruh and V. Radisavljevic, *MODELING OF CLOSED KINEMATIC CHAINS WITH FLEXIBLE LINKS*, Department of Mechanical and Aerospace Engineering, Rutgers University.

[17] H. Baruh, *Analytical Dynamics*, WCB McGraw-Hill, 1999.

[18] A. Isidori, *Nonlinear Control Systems*, Springer, 3rd ed. 1995.